New Fluorescent Octadecapentaenoic Acids as Probes of Lipid Membranes and Protein-Lipid Interactions

C. Reyes Mateo,* Andre A. Souto,*# Francisco Amat-Guerri,# and A. Ulises Acuña*
*Instituto de Química-Física "Rocasolano," C.S.I.C., and #Instituto de Química Orgánica, C.S.I.C., E-28006 Madrid, Spain

ABSTRACT The chemical and spectroscopic properties of the new fluorescent acids all(*E*)-8,10,12,14,16-octadecapentaenoic acid (*t*-COPA) and its (8*Z*)-isomer (*c*-COPA) have been characterized in solvents of different polarity, synthetic lipid bilayers, and lipid/protein systems. These compounds are reasonably photostable in solution, present an intense UV absorption band ($\epsilon_{350\ nm} \approx 10^5\ M^{-1}\ cm^{-1}$) strongly overlapped by tryptophan fluorescence, and their emission, centered at 470 nm, is strongly polarized ($r_0 = 0.385 \pm 0.005$) and decays with a major component (85%) of lifetime 23 ns and a faster minor one of lifetime 2 ns (D,L-α-dimyristoylphosphatidylcholine (DMPC), 15°C). Both COPA isomers incorporate readily into vesicles and membranes ($K_p \approx 10^6$) and align parallel to the lipids. *t*-COPA distributes homogeneously between gel and fluid lipid domains and the changes in polarization accurately reflect the lipid T_m values. From the decay of the fluorescence anisotropy in spherical bilayers of DMPC and POPC it is shown that *t*-COPA also correctly reflects the lipid order parameters, determined by ^2H NMR techniques. Resonance energy transfer from tryptophan to the bound pentaenoic acid in serum albumin in solution, and from the tryptophan residues of gramicidin in lipid bilayers also containing the pentaenoic acid, show that this probe is a useful acceptor of protein tryptophan excitation, with R_0 values of 30–34 Å.

INTRODUCTION

Physicochemical aspects of lipid organization in model and biological membranes, as well as of the interaction between lipids and both integral and extrinsic membrane proteins, can often be usefully investigated by means of fluorescent fatty acids and lipids (see, e.g., Hudson et al., 1986; Hudson and Cavalier, 1988) that have the important advantage that the superstructure being probed is minimally perturbed. The utility of such lipid analog probes resides in the sensitivity of some of their spectral parameters to the microenvironment. Sklar et al. (1977a,b) introduced the naturally occurring 18-carbon fluorescent lipid analog *trans*-parinaric acid (*t*-PnA), which contains a linear conjugated all(*E*)-tetraene chromophore, and since then it has been used fruitfully in the applications mentioned above (see, e.g., Ruggiero and Hudson, 1989a,b; Lentz, 1993; Mateo et al., 1993a, 1995). In many cases the choice of *t*-PnA is based on the sensitivity of its fluorescence kinetics to the intriguing preferential solubility of this compound for gel-like lipid regions (Sklar et al., 1977b; Sklar, 1980). On the other hand, some of the potential applications of *t*-PnA as a probe might be prevented by this specific concentration effect. The technique of resonance energy transfer (RET) involving lipophilic fluorescent probes has also been used with success in studies of lipid-protein and membrane-protein interactions (for a recent review see Van der Meer et al., 1994). In cases where the tryptophan residues of the protein act as donors, the tetraene *t*-PnA may be used as a nonperturbing acceptor partner in the bilayer (Kimelman et al., 1979). However, the proximity of the absorption band of *trans*-parinaric acid, centered at ~314 nm, and its strong overlap with those of the tryptophan fluorescence spectrum impose quite severe experimental difficulties.

To remove these limitations and, at the same time, to extend the possible choices of fluorescent lipid analogs, we have synthesized (Souto et al., 1994) a new set of conjugated polyene derivatives that contain a linear pentaene system. Two representative members are the conjugated fatty acid all(*E*)-8,10,12,14,16-octadecapentaenoic acid (*t*-COPA) and its (8*Z*)-isomer (*c*-COPA), depicted in Fig. 1. In the present work we show that, compared with the well-known parinaric acid probe, the extra double bond of both COPA isomers shifts both the absorption and emission spectra to the red, increases the absorption coefficient and the fluorescence lifetime, and augments the molecular rigidity. As a consequence, these pentaenoic fatty acids are extremely good acceptors of the electronic excitation energy of tryptophan residues, facilitating the use of RET for studies of protein-lipid interactions and proximity relationships, and they accurately reflect the average lipid and membrane order parameters and transition temperatures, because their spectral properties are not affected by environmental thermal changes in the 10–40°C range. In addition to the basic photophysical parameters of the COPA isomers, we report here several prototypical examples of the use of the time-resolved fluorescence depolarization of these pentaenoic acids to probe the structure and dynamics of DMPC and POPC lipid bilayers, as well as that of RET to monitor the interaction of said acids with proteins in solution and, in membranes, with membrane-bound peptides, indicating the advantages and limitations of these new fluorescent lipid probes in membrane research.

Received for publication 14 March 1996 and in final form 8 July 1996.
Address reprint requests to Dr. A. Ulises Acuña, Instituto de Química-Física "Rocasolano," C.S.I.C., Serrano 119, E-28006 Madrid, Spain. Tel.: 34-1-5619400; Fax: 34-1-5642431; E-mail: roculises@roca.csic.es.

0006-3495/96/10/2177/15 $2.00

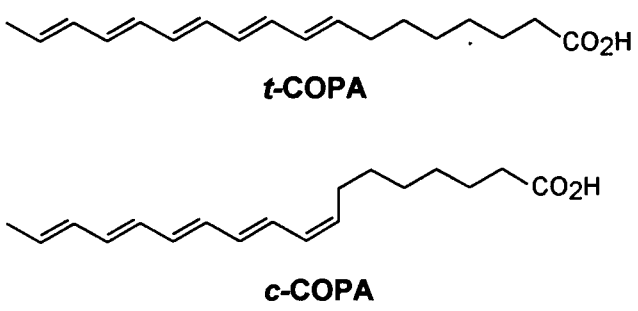

FIGURE 1 Structure of all(*E*)-8,10,12,14,16-octadecapentaenoic acid (*t*-COPA) and its (8*Z*)-isomer (*c*-COPA).

MATERIALS AND METHODS

Materials

The fluorescent conjugated pentaenoic acid all(*E*)-8,10,12,14,16-octadecapentaenoic acid (*t*-COPA) and its (8*Z*)-isomer (*c*-COPA) were synthesized and purified as described elsewhere (Souto et al., 1994). The all(*E*)-tetraene *trans*-parinaric acid (*t*-PnA) was purchased from Molecular Probes (Eugene, OR) and checked by absorption and emission spectroscopy and by high-performance liquid chromatography. The spin probes 5-doxyl-stearic acid (5NS) and 16-doxyl-stearic acid (16NS), from Sigma Chemical Co. (St. Louis, MO), were used without further purification. The synthetic phospholipids D,L-α-dimyristoylphosphatidylcholine (DMPC), D,L-α-dipalmitoylphosphatidylcholine (DPPC), and L-α-(β-oleoyl-γ-palmitoyl)phosphatidylcholine (POPC), as well as human serum albumin (HSA) and gramicidin D, were obtained from Sigma Chemical Co. Gramicidin D (also named in some cases gramicidin A′) is a 80:5:15 natural mixture of gramicidin A, B, and C, respectively, with four (A) and three (B and C) tryptophan residues. The paraffin oil PRIMOL 352 (Exxon, viscosity at 20°C = 1.9 poise) was free of fluorescent contaminants in the wavelength range of interest (>340 nm) and was used as received.

Multilamellar vesicles (MLVs) were prepared at 0.25 mg/ml phospholipid concentration by suspending the appropriate amount of the dried lipid in distilled water or in 10 mM Tris/HCl (pH = 7), heating the suspension above the phase transition temperature, and vortexing. Large unilamellar vesicles (LUVs) with a mean diameter of 90 nm were prepared from the multilamellar suspension by extrusion (Hope et al., 1985) through 0.1-μm polycarbonate filters (Nucleopore, Cambridge, MA).

Stock solutions of the fluorescent COPA compounds (10^{-4} M) or of the spin probes (10^{-3} M) were prepared in ethanol (spectroscopic grade), using ultrasonic mixing in the case of the COPA probes. The solutions of the fluorescent compounds were saturated with argon and stored in the dark. A few microliters of these solutions were added to several milliliters of vesicle suspensions to obtain a probe/lipid molar ratio of ~1:200, which were then stirred above the lipid transition temperature. The spectroscopic measurements were made immediately after preparation.

Gramicidin D was incorporated into MLVs as described previously (Mukherjee and Chattopadhyay, 1994). Briefly, a peptide/lipid mixture (1:140 molar ratio) was codissolved in methanol with a few drops of chloroform, dried under nitrogen, hydrated with 10 mM sodium phosphate buffer (pH 7.2, 150 mM NaCl), and vortexed to obtain MLVs and, subsequently, LUVs. The samples were incubated overnight at 65°C with continuous stirring to induce the channel-forming β-helical monomeric conformation (Lograsso et al., 1988; Bañó et al., 1991).

Human platelets, isolated from outdated and purified fragments of the platelet plasma membrane, were prepared as described elsewhere (Mateo et al., 1991).

Calorimetric measurements

Thermograms of the calorimetric phase transition of lipid multilamellar vesicles were recorded by differential scanning calorimetry (DSC) in a Microcal MC-2 instrument. All experiments were performed with a scan rate of 1 K·min^{-1}.

Absorption and fluorescence spectroscopy

Absorption spectra were registered in a CARY 219 spectrophotometer (Varian). Fluorescence spectra and steady-state anisotropy $\langle r \rangle$ were recorded with a SLM-8000D fluorimeter fitted with Glan polarizers. Fluorescence quantum yields (Φ_F) were determined by reference to quinine sulfate in 0.05 M H_2SO_4 ($\Phi_F = 0.51$; Velapoldi, 1972). The time-resolved measurements were carried out by recording the decay of the observed parallel $I_{\parallel}(t)$ and perpendicular $I_{\perp}(t)$ components and that of the total intensity $I_{55}(t)$ of the fluorescence elicited by vertically polarized excitation, in a time-correlated single-photon-counting spectrometer (Mateo et al., 1991). The samples were excited at 337 nm with a thyratron-gated nanosecond flash lamp (Edinburgh Inst., EI199) filled with nitrogen. The emission was isolated with a 408-nm cutoff filter (Schott KV) and detected with a Phillips XP2020Q photomultiplier.

The kinetic parameters of the decay of the fluorescence intensity (lifetimes, τ_i, and amplitudes, a_i) and of the anisotropy decay (rotational correlation times, ϕ_i, amplitudes, β_i, and residual anisotropy, r_∞) were determined using nonlinear least-squares regression methods (see Mateo et al., 1991) developed from published descriptions (Knutson et al., 1983; Cross and Fleming, 1984; Löfroth, 1985). In both cases the fits tabulated here represent the minimum set of adjustable parameters that satisfy the usual statistical criteria, namely a reduced χ^2 value of <1.3 and a random distribution of weighted residuals.

Analysis of the fluorescence anisotropy

The decay of the emission anisotropy $r(t)$ of COPA in lipid vesicles was formally approximated by a sum of n exponentials and a constant term (Dale et al., 1977; Heyn, 1989):

$$r(t) = (r(0) - r_\infty)\left[\sum_{i=1}^{n} \beta_i \exp(-t/\phi_i)\right] + r_\infty, \qquad (1)$$

where $\sum_{i=1}^{n} \beta_i = 1$ and $n = 1$, 2, or 3.

In most cases (see below) the initial anisotropy $r(0)$ was fixed in the numerical analysis to the value determined in very viscous solution (glycerol at −30°C) from steady-state techniques, $r_0 = 0.385 \pm 0.005$. The residual anisotropy r_∞, in the case of a cylindrically symmetric chromophore in a suspension of lipid vesicles, is related (Naqvi and Acuña, 1992) to the average order parameter of the probe, S, relative to its local director by

$$r_\infty = (2/5)P_2(\cos\theta_a)P_2(\cos\theta_e) \cdot S \cdot S^*, \qquad (2)$$

where $P_2(x)$ are the Legendre polynomials for the angles θ_a and θ_e between the absorption and emission transition moments and the unique inertial axis of the probe, and S and S^* are the order parameters of the probe in the ground and electronically excited states, respectively (Naqvi, 1980, 1981). If the chromophore transition moments are colinear and do not depart greatly from the probe axis, the above expression approximates well a more compact form that can be further simplified, if $S^* \approx S$, to

$$r_\infty = r_0 \cdot S^2. \qquad (3)$$

A detailed discussion of the physical concepts underlying Eq. 3 has recently been published (Toptygin and Brand, 1995).

To compare the time-dependent reorientational mobility in lipid bilayers of the new fluorescent chromophores described here with that of other

well-characterized membrane probes, we determined the rotational diffusion constant about the axis perpendicular to the molecular axis $D_\perp$ and the "apparent viscosity" η of the bilayer with *t*-COPA. For this purpose we have assumed the simplest model for the Brownian diffusion of a rodlike probe in an angular potential (Kinosita et al., 1977, 1984), where the decay of the anisotropy is approximated by an exponential function (Lipari and Szabo, 1980) with an average relaxation time $\langle\phi\rangle$ for returning to the initial equilibrium distribution:

$$r(t) = (r_0 - r_\infty) \exp(-t/\langle\phi\rangle) + r_\infty. \quad (4)$$

It is worth noting that Brownian dynamics simulations of the restricted motion of a rod in different orienting potentials (López and García de la Torre, 1987) predict anisotropy decays for which this simple model recovers the rotational diffusion constant $D_\perp$ with unexpected accuracy (average deviation < 15%).

In the present case, the experimental values of $\langle\phi\rangle$ were obtained from the area under the anisotropy decay curve (Kinosita et al., 1977, 1984):

$$\langle\phi\rangle = \int_0^\infty (r(t) - r_\infty)/(r_0 - r_\infty))\mathrm{d}t = \sum_i^n \beta_i\phi_i. \quad (5)$$

According to the model, $\langle\phi\rangle$ is a function of $D_\perp$ and of a parameter σ related to the potential that restricts the probe reorientation:

$$\langle\phi\rangle = \frac{\sigma}{D_\perp} \quad (6)$$

Numerical values of σ as a function of r_∞/r_0 have been tabulated (Kinosita et al., 1977, 1984) or can be computed from analytical expressions (Lipari and Szabo, 1980). In this work we used those for a Gaussian-shaped angular potential, σ_G (Engel and Prendergast, 1981; Kinosita et al., 1982), which seems physically more realistic than the standard hard-cone model. It was computed from a polynomial approximation to the data of Kinosita et al. (1982) as a function of the experimentally determined r_∞/r_0 value:

$$\sigma_G = 0.1674 - 0.1066(r_\infty/r_0) - 0.062(r_\infty/r_0)^2. \quad (7)$$

The experimental $D_\perp$ value for the lipid probe can therefore be obtained from Eqs. 6 and 7, and in turn, a semiquantitative estimate can be made of the rotational drag acting on the probe within the hydrocarbon core of the bilayer. This is usually expressed in terms of the viscosity (η) of the paraffin oil, which would give rise to the same numerical value of the probe rotational diffusion coefficient $D_\perp$ that was found in the bilayer. The limitations of this "equivalent viscosity" are well known and have recently been discussed in detail (Best et al., 1987; Van der Meer, 1991; Valeur, 1993).

The relationship between $D_\perp$ and the viscosity in an isotropic solvent is conveniently expressed by a modified form (Dote et al., 1981; Mateo et al., 1993b) of the Stokes-Einstein-Debye equation:

$$D_\perp = \frac{k_B T}{6\eta f_\perp V g_\perp}, \quad (8)$$

where V is the hydrodynamic volume, $g_\perp$ is the classical Perrin shape factor that takes into account the asymmetry of the rotating object, and $f_\perp$ is a dimensionless factor that depends on the friction mechanism. For "stick" boundary conditions $f = 1$, and the value of the rotational coefficient would correspond to D (stick). If the boundary conditions are intermediate between slip and stick, f values will be less than 1 (Hu and Zwanzig, 1974), yielding a higher value for the rotational coefficient, D (slip). When the conformation in solution of the rotating molecule is known, V may be taken as the van der Waals volume. However, the specific mechanism of the rotational friction (slip/partial slip/stick) must be determined experimentally.

Fluorescence quenching

Fluorescence quenching measurements of the pentaenoic acids by spin probes in lipid bilayers were analyzed by Stern-Volmer plots of I_0/I versus the quencher concentration in the lipid phase $[Q_L]$. If $K_P = [Q]_L/[Q]_A$ is the molar partition coefficient of the quencher between the lipid and the aqueous phases, $[Q]_L$ is given by:

$$[Q]_L = \frac{K_P V_T}{V_A + V_L K_P}[Q]_T, \quad (9)$$

where $[Q]_T$ is the concentration of quencher in the total volume $V_T = V_L + V_A$, and V_L and V_A are, respectively, the volume of the lipid and the aqueous phase (see Castanho and Prieto, 1995).

For 5NS and 16NS, the partition coefficients for the lipid fluid phase are 89,000 and 9730, respectively, and for the gel phase 12,570 and 3340, respectively (Wardlaw et al., 1987).

Radiationless electronic energy transfer

For a donor-acceptor pair with a fixed relative distance R_{da}, the efficiency of resonance electronic energy transfer, E, is given by

$$E = R_0^6/(R_0^6 + R_{da}^6), \quad (10)$$

where R_0 is the donor-acceptor distance at which the transfer efficiency is 50%. R_0 is expressed (Förster, 1959) by

$$R_0^6 = \frac{9000(\ln 10)\kappa^2\Phi_D J}{128\pi^5 n^4 N_A}, \quad (11)$$

where Φ_D is the donor quantum yield in the absence of acceptor molecules, n is the refractive index of the medium, N_A is the Avogadro constant, κ^2 is the orientation factor, and J is the overlap integral between the donor emission and the acceptor absorption spectra. J is given by

$$J = \int_0^\infty f_D(\lambda)\epsilon_A(\lambda)\lambda^4 \,\mathrm{d}\lambda, \quad (12)$$

where λ is the wavelength, ϵ_A is the molar absorption coefficient of the acceptor at that λ, and $f_D(\lambda)$ is the fluorescence spectrum of the donor normalized to unit area on the wavelength scale.

RESULTS

Isotropic solvents

Absorption spectroscopy

The absorption spectra of *t*- and *c*-COPA show characteristic structured shapes between 270 and 360 nm (Fig. 2). These shapes are similar to those observed for *t*-PnA and its *cis* isomer but shifted ~30 nm to the red, and both spectra shift to longer wavelengths on increasing solvent polarizability, as in the case of these tetraenes (Sklar et al., 1977a) as well as other polyenes (Hudson et al., 1982). The peak positions of the absorption bands in several solvents are listed in Table 1 together with the molar absorption coefficients. The values of these coefficients in hexane and chloroform appear to be abnormally low, probably because of the incomplete solubilization of the fluorescent derivatives in those solvents.

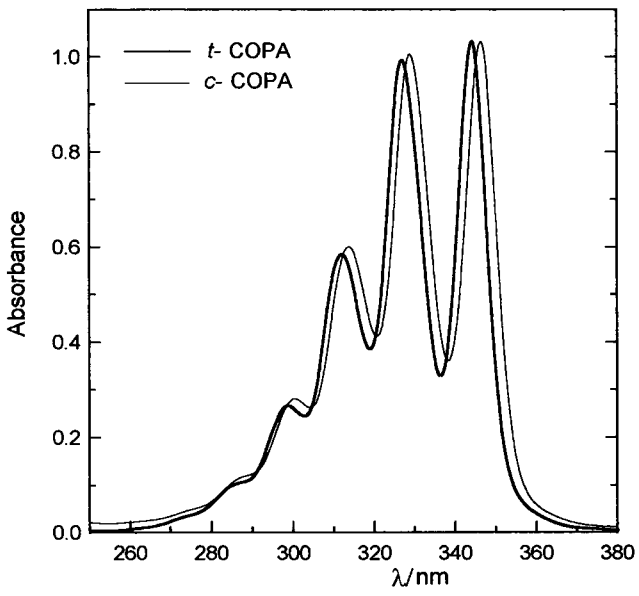

FIGURE 2 Absorption spectra of *t*-COPA (*bold curve*) and *c*-COPA (*thin curve*), 10^{-6} M in ethanol at 20°C.

Steady-state fluorescence

The fluorescence emission of both COPA isomers in solvents of medium polarity consists of a wide, structureless band (Fig. 3) with a large Stokes shift of ~7000 cm^{-1} and a moderate quantum efficiency (Table 1). In ethanol solution, the fluorescence yield increased by a factor of 2 on deoxygenation. The emission maxima of both *trans* and *cis* isomers are well separated from their absorption maxima, appearing at 468 and 474 nm, respectively, and these positions are independent of the solvent polarizability, as is the case in other polyenes. In water and saline buffers, the solubility of these compounds is extremely low and, therefore, the fluorescence is almost undetectable. In aerated ethanol solution both isomers are thermally stable, and the fluorescence intensity under steady illumination (2-nm slits) is unchanged for several hours. Under intense UV irradiation (16-nm slits, 3 h) a 10% decrease in the fluorescence intensity of *t*-COPA is observed; a similar solution of *t*-PnA is photodegraded to the same extent in ~30 min. In viscous solvents (Fig. 3) the fluorescence emission is strongly polarized and the value of the anisotropy remains constant through the near-UV excitation and the fluorescence spectra, when recorded in ethylenglycol at −27°C. In these conditions, the fluorophore still retains some rotational mobility. In glycerol at −30°C the anisotropy rises to a maximum value of $r_0 = 0.385 \pm 0.005$ for the two isomers and did not increase when the temperature was lowered further.

Kinetics of the fluorescence intensity and anisotropy

The decay of the fluorescence emission of the two isomers in the solvents detailed in Table 2 is clearly biexponential, consisting of a major kinetic component (90–95%) with a long lifetime and a small contribution of a faster component (original data and fitting shown in Fig. 4 for the ethanol solution of *t*-COPA). On degassing the ethanol solution of each isomer, both lifetimes increased by roughly a factor of 2, as did the stationary fluorescence yield. The values of the lifetimes listed in Table 2 arise subject to oxygen quenching. Because the two lifetimes are quenched to the same extent (~50%), the oxygen quenching rate constant (~10^{10} M^{-1} s^{-1}) is apparently twice as large for the short as for the long lifetime. Interestingly, the decay parameters show only a weak dependence on temperature, in the 20–40°C range, in contrast with the behavior of the tetraene *t*-PnA (Sklar et al., 1977a; Mateo et al., 1993a). The average radiationless rate constant, k_{nr}, and radiative lifetime, τ_r, can be estimated from the fluorescence quantum yield of the ethanol solution (at 22°C) and the average lifetime, using standard expressions. The plot of ln k_{nr} versus $1/T$ for the data of *t*-COPA in ethanol and paraffin oil solutions (Fig. 4, *inset*) shows an Arrhenius-type behavior, with an activation energy for the overall radiationless processes of 1.0 ± 0.1 kcal·mol^{-1}.

The decay of the emission anisotropy of *t*-COPA in the viscous paraffin oil was analyzed in the 20–40°C temperature range. The experimental curves (see, e.g., Fig. 5) were fitted to a three-exponential function (Table 4), with the value of $r(0)$ fixed at 0.385 (see above). The fast subnanosecond correlation time ϕ_1 is poorly defined, because of the limited time resolution of the spectrometer used here. The tabulated data show that the three correlation times decrease at higher temperatures (lower viscosity), and that the coefficient of the slowest correlation time ϕ_3 remains independent of the temperature, as would be expected for rigid-body rotational depolarizing motions. Moreover, a plot of ϕ_3 versus η/T (Fig. 5, *inset*) for *t*-COPA is linear in this temperature range and extrapolates through zero, indicating regular hydrodynamic behavior. In contrast, the preexponential coefficients of ϕ_1 and ϕ_2 change significantly with increased temperature.

Lipid bilayers

Probe partitioning

The incorporation of *t*- and *c*-COPA into the lipid bilayers is very fast, taking place in a few minutes if the lipid is in the fluid phase. LUVs of DMPC were used to determine the partition of the probe between the aqueous buffer and the gel and fluid lipid phases. Because the fluorescence emission of the probe in water is almost negligible and becomes much more intense when it is dissolved in the bilayer, the incorporation of the probe into DMPC was quantitated by the fluorescence technique of Sklar (1980). In these experiments, the lipid concentration was varied while the probe concentration was kept constant. The molar partition coefficients between the lipidic gel phase and the aqueous phase, K_p^G, of *t*- and *c*-COPA, determined at 10°C, were (0.7 ± 0.1) × 10^6 and (2.5 ± 0.4) × 10^6, respectively. The cor-

TABLE 1 Absorption and fluorescence of *t*-COPA and *c*-COPA in solution and in lipid bilayers at 22°C

	Solvent	n*	λa_{max} (nm) (±0.3)	λem_{max} (nm) (±1)	ϵ_{max} ($M^{-1} \cdot cm^{-1}$) (±2000)	Φ_F (±10%)
t-COPA	Hexane	1.375	344.3	468	(68,000)#	
	Ethanol	1.361	344.7	468	103,000	0.075
	Ethanol($-O_2$)§		344.7	468		0.15
	THF	1.405	348.0	468		
	Dioxane	1.416	348.9	468	81,400	0.14
	Chloroform	1.446	351.3	468	(75,000)#	
	Paraffin oil	1.470¶	349.0	468		~0.13‖
	Glycerol	1.475	352.0	468		
	DMPC (30°C)		349.0	468		~0.1‖
	DMPC (17°C)		350.5	468		~0.1‖
c-COPA	Ethanol		347.0	474	108,000	0.084
	Ethanol($-O_2$)§		347.0	474		0.14
	Dioxane		351.5	474	81,500	0.12
	Chloroform		353.5	474	(53,200)#	
	Glycerol		353.5	474		
	DMPC (30°C)		350.5	474		~0.1‖
	DMPC (17°C)		352.0	474		~0.1‖

*Refractive index n_D^{20}, data taken from *CRC Handbook of Chemistry and Physics*, 73rd. Ed. 1992. CRC Press, Boca Raton, FL 8–49.
#Probably incomplete solubilization.
§Degassed by argon bubbling.
¶ This work.
‖Estimated from the average lifetime.

responding partition coefficients between the fluid lipid phase and the aqueous phase, K_p^F, determined at 30°C, were $(0.5 \pm 0.1) \times 10^6$ and $(1.8 \pm 0.4) \times 10^6$.

The partition coefficient of these fluorophors between the gel and fluid phases of the lipid, $K_p^{G/F}$, can be estimated from the above values by $K_p^{G/F} = K_p^G/K_p^F$ (Sklar et al., 1979). Accordingly, it results that $K_p^{G/F} = 1.4 \pm 0.4$ for *t*- and *c*-COPA, indicating that neither isomer has a specific preference for either of the two lipid phases.

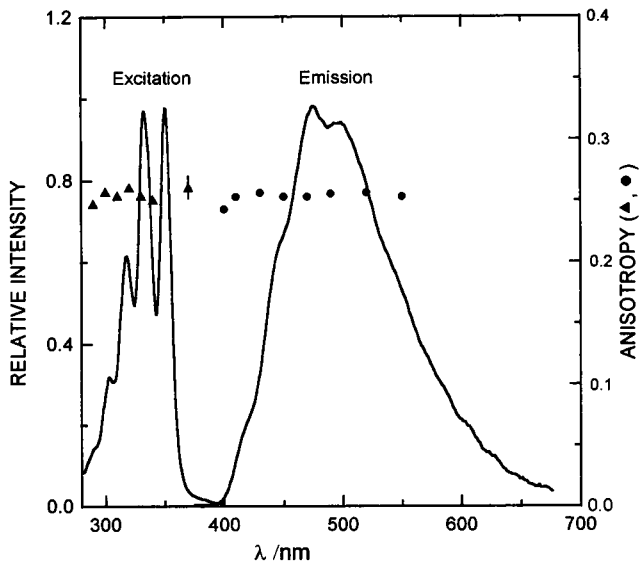

FIGURE 3 Corrected fluorescence excitation (*thin curve*) and emission (*bold curve*) spectra of *t*-COPA in chloroform. The fluorescence excitation (▲) and emission (●) anisotropies in ethyleneglycol at −27°C are also displayed.

Transverse location in the bilayer

Considering the fatty-acid-like character of COPAs, the most likely arrangement of these compounds in a lipid bilayer would be roughly parallel to the lipid chains. An experimental check of this expectation was carried out by monitoring the relative quenching of the fluorescence of both isomers by the lipophilic spin probes 5NS and 16NS, in which the nitroxide group is located at 12 Å and 3 Å, respectively, from the bilayer center (Chattopadhyay and London, 1987). The Stern-Volmer plots of the fluorescence changes for *t*-COPA in LUVs of DMPC in the ordered (17°C) and fluid (30°C) phases are shown in Fig. 6. The ratio of the average quenching constants $K_{SV(16NS)}/K_{SV(5NS)}$ is ~3 for the fluid phase and 5 for the gel, for the two COPA isomers. Although very detailed methods have been developed to analyze this kind of experiment (see, e.g., Chattopadhyay and London, 1987; Castanho and Prieto, 1995; Castanho et al., 1996), for our purposes here, the direct comparison of the quenching constants provides a qualitative confirmation of the expected location of the COPA chromophore, buried deep within the bilayer and away from the lipid/water interface. The lower ratio of the quenching constants in the fluid phase is probably due to the greater transverse fluctuations of the fluorophore and/or the quenchers.

TABLE 2 Fluorescence kinetic parameters of *t*-COPA and *c*-COPA in isotropic solutions

	Solvent	T (°C)	a_1 (±0.03)	τ_1 (ns) (±0.5)	a_2 (±0.03)	τ_2 (ns) (±0.3)	$\langle\tau\rangle$ (ns)*	τ_r (ns) (±20)	k_{nr} ($10^7 \cdot s^{-1}$) (±0.7)
t-COPA	Ethanol	20	0.10	4.1	0.90	11.4	10.7	143	8.6
		30	0.09	2.9	0.91	10.9	10.2	143	9.1
		40	0.10	2.9	0.90	10.4	9.7	143	9.5
	Ethanol($-O_2$)#	20	0.11	10.1	0.89	21.5	20.3	135	4.2
	Dioxane	20	0.09	6.0	0.91	14.5	13.7	100	6.3
	Paraffin oil	22	0.04	4.7	0.96	19.4	18.8	143§	4.6
		30	0.06	5.0	0.94	18.8	17.8	143§	4.9
		39	0.04	3.3	0.96	17.7	17.1	143§	5.1
c-COPA	Ethanol	20	0.11	4.1	0.89	10.9	10.2	121	9.0
	Ethanol($-O_2$)#	20	0.13	9.7	0.87	19.3	18.1		
	Paraffin oil	22	0.06	5.7	0.94	17.2	16.5		
		30	0.07	6.5	0.93	16.7	16.0		
		39	0.06	5.7	0.94	16.0	15.4		

*Average lifetime $\langle\tau\rangle = a_1 \cdot \tau_1 + a_2 \cdot \tau_2$.
#Degassed.
§Assuming the same value as in ethanol solution.

Perturbation of bilayer structure

The effect of *t*- and *c*-COPA on the thermotropic behavior of lipids in MLVs of DPPC containing increasing amounts of the fluorescent probe was studied by DSC in the heating mode. The thermograms of DPPC vesicles containing the probe were virtually identical to that of the pure lipid, even for probe concentrations as high as 10 mol% (Fig. 7). The main phase transition temperature, T_m, was 41.31°C for pure DPPC vesicles and 41.26 ± 0.06°C for lipid/*t*-COPA molar ratios of 50, 30, and 10. The shape and location of the pretransition was also coincident with that of the pure lipid, and only in the case of *c*-COPA was the width of the thermal phase transition broadened slightly at lipid/probe ≤ 10. This demonstrates that neither probe disrupts the overall structure of the lipid bilayer, a result that might be expected in view of the fatty acid character of these compounds.

Detection of lipid phase transitions

As shown above, the fluorescence intensity of both COPA isomers is only weakly temperature dependent around ambient. Because these compounds do not perturb the lipid bilayer structure, their emission polarizations should accu-

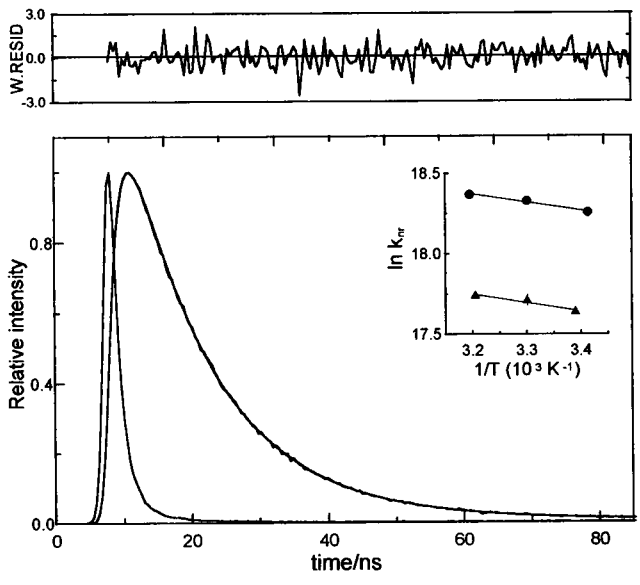

FIGURE 4 Decay of the fluorescence intensity of an ethanol solution of *t*-COPA (10^{-6} M, 20°C). The experimental data were fitted to a double-exponential function with the parameters listed in Table 2. (*Inset*) Arrhenius plot of the average radiationless rate (k_{nr}) of *t*-COPA in ethanol (●) and paraffin oil (△).

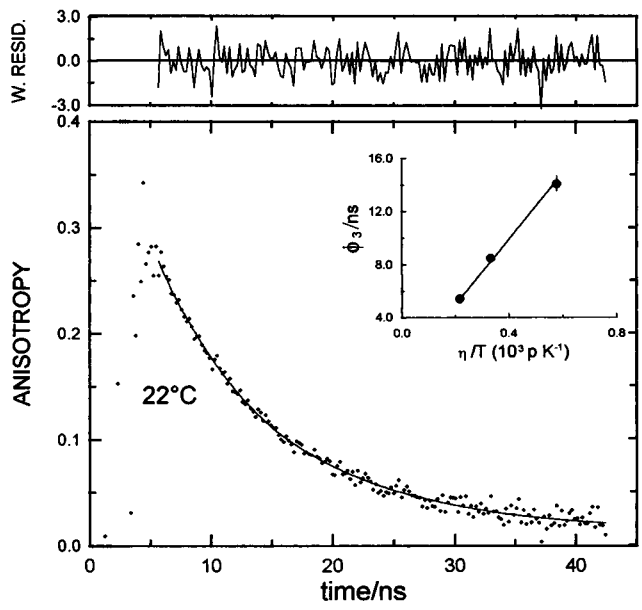

FIGURE 5 Time-resolved fluorescence anisotropy of *t*-COPA in paraffin oil at 22°C (see Table 4 for decay parameters). (*Inset*) Variation of the slower correlation time ϕ_3 as a function of η/T.

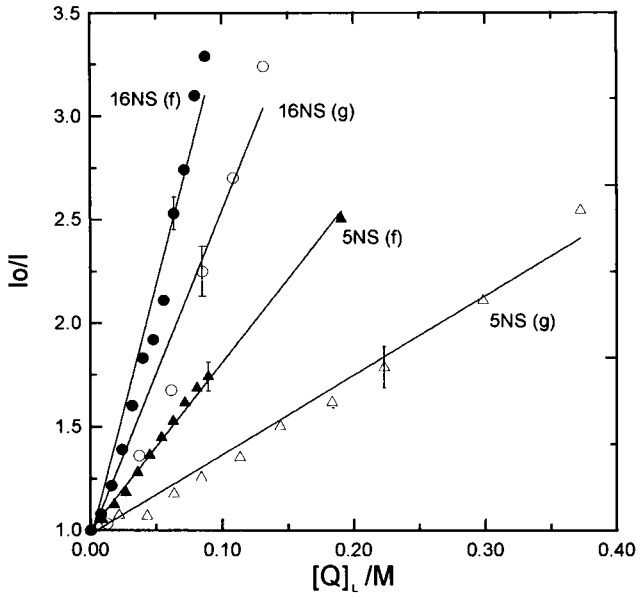

FIGURE 6 Stern-Volmer plot for the quenching of *t*-COPA by the spin probes 5NS and 16NS in unilamellar vesicles of DMPC at 17°C (gel phase) and 30°C (fluid phase).

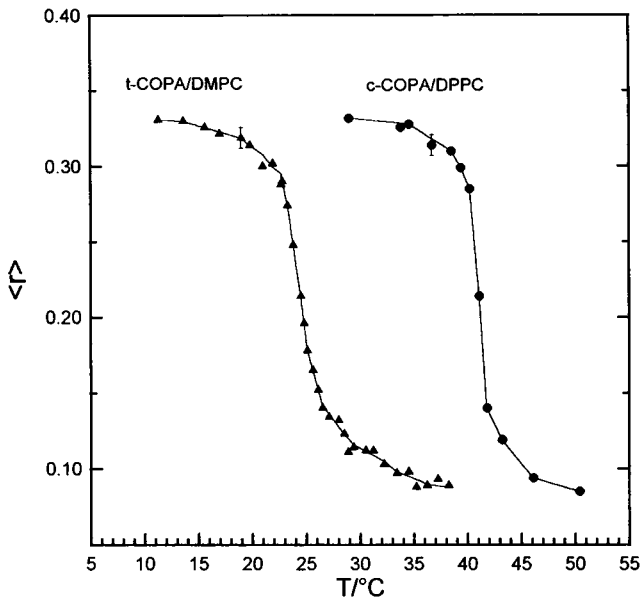

FIGURE 8 Variation of the steady-state fluorescence anisotropy, $\langle r \rangle$, with temperature for *t*-COPA in large unilamellar vesicles of DMPC (T_m = 23°C), and for *c*-COPA in unilamellar vesicles of DPPC (T_m = 41°C).

rately reflect the lipid thermal transitions. This is in fact observed when the steady-state anisotropy $\langle r \rangle$ of the COPA isomers is recorded in LUVs of DMPC and DPPC. As can be seen in Fig. 8, the value of $\langle r \rangle$ changes only slowly both above and below the phase transition, and a very large, sharp change is observed at the transition temperature. The T_m values obtained from the variation in the fluorescence polarization of the COPA probes are in excellent agreement with previous calorimetric data (Mabrey and Sturtevant, 1976), as well as with those determined in this work by DSC.

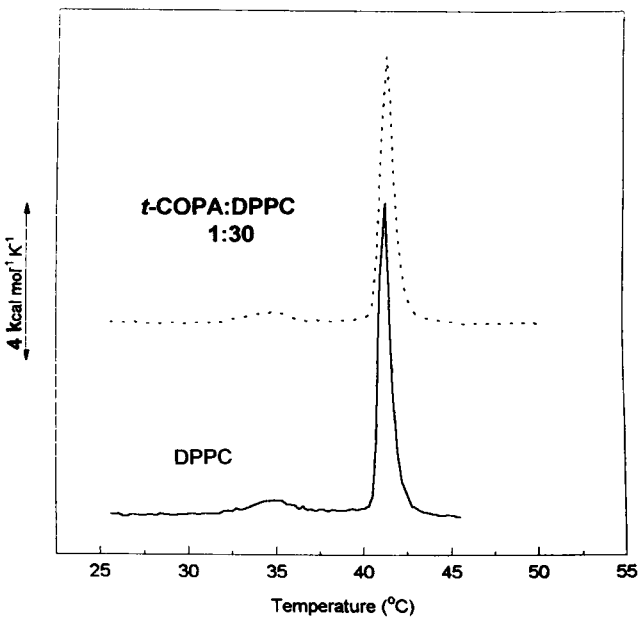

FIGURE 7 Differential scanning calorimetry thermograms of multilamellar vesicles of pure DPPC, and with 3.3 mol% *t*-COPA.

Time-resolved fluorescence intensity and anisotropy

The decay of the fluorescence intensity of the two COPA isomers was studied in lipid bilayers (LUVs) as a function of temperature in the ordered and fluid phases for DMPC, and in the fluid phase for the unsaturated lipid POPC. The decay could be fitted in most cases to a two-exponential function, although occasionally a third, faster component (1–2 ns) improved the fitting statistics, particularly at the higher temperatures (Table 3). These data show that a major fraction of the decay (70–90%) relaxes through the longest lifetime component, which is not very different from that recorded in the paraffin oil (Table 2), although its relative weight is less than in the viscous solvent. The fractional weight of the fastest (and intermediate, if present) lifetimes is virtually independent of the temperature in this range, as would be expected from the weak thermal dependence of the average k_{nr} noted before. In addition, degassing of the POPC vesicle suspension had no effect on the lifetime values. It is also shown here that the excited-state kinetics of these compounds is not sensitive to the large structural changes taking place at the lipid phase transition. This is in stark contrast with what has been observed for the tetraene analog *t*-PnA (Sklar et al., 1977a; Hudson et al., 1986; Mateo et al., 1993a).

The decay of the fluorescence anisotropy was also studied in DMPC and POPC lipid vesicles, over the same temperature range as above. Representative experimental

TABLE 3 Fluorescence kinetic parameters of *t*-COPA and *c*-COPA in large unilamellar lipid vesicles of DMPC and POPC

	Lipid	T (°C)	a_1 (±0.03)	τ_1 (ns) (±0.5)	a_2 (±0.03)	τ_2 (ns) (±0.5)	a_3 (±0.03)	τ_3 (ns) (±0.5)	χ^2
t-COPA	DMPC	15	0.15	2.0	—	—	0.85	23.0	1.09
		25	0.15	2.2	—	—	0.85	20.0	1.19
		30	0.16	2.3	—	—	0.84	19.1	1.22
			0.13	1.0	0.09	5.1	0.78	19.5	1.14
		40	0.18	3.6	—	—	0.82	18.3	1.30
			0.23	0.8	0.13	6.3	0.65	18.8	1.16
	POPC	10	0.07	2.4	0.08	9.6	0.85	21.9	1.13
		15	0.10	0.9	0.11	9.3	0.79	21.5	1.17
		20	0.07	1.4	0.13	9.5	0.80	20.8	1.20
		25	0.10	1.3	0.13	9.5	0.77	20.3	1.21
		30	0.06	1.7	0.14	8.7	0.80	19.6	1.25
		40	0.14	0.9	0.18	9.6	0.68	18.9	1.20
	POPC($-O_2$)*	20	0.08	1.0	0.17	9.3	0.75	22.3	1.20
c-COPA	DMPC	15	0.08	3.7	0.92	18.7			1.04
		25	0.11	3.8	0.89	17.2			1.08
		30	0.09	3.7	0.91	16.7			1.19
		40	0.12	4.8	0.88	16.5			1.29

*Degassed.

curves for *t*-COPA, recorded below and above the phase transition of DMPC, are shown in Fig. 9, where it can be seen that the anisotropy decays in a few to a few tens of nanoseconds to a residual, time-independent value, which is

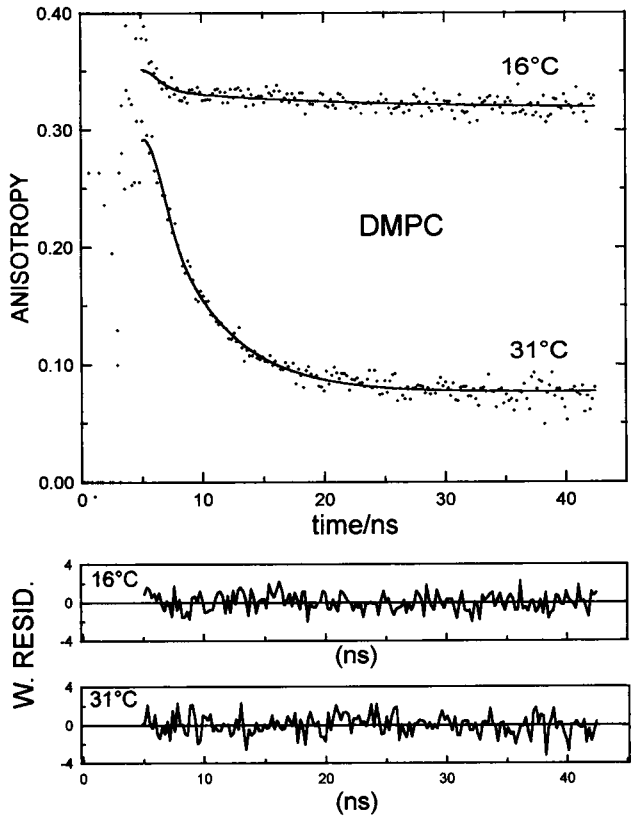

FIGURE 9 Time-resolved fluorescence anisotropy of *t*-COPA in unilamellar vesicles of DMPC in the gel (16°C) and fluid (31°C) phases (see Table 4 for decay parameters).

widely different for the two lipid phases. The results of the deconvolution analysis of all the data sets, carried out by taking the $r(0)$ value as a constant fixed at 0.385, are listed in Table 4. When these probes are embedded in the ordered lipid phase, the r_∞ value is ~80% of this initial anisotropy value. To adequately fit the small kinetic component in these conditions, two rotational correlation times are needed; one of them is in the subnanosecond time range and, therefore, is ill-defined. In the fluid phase, most of the $r(t)$ decay data required two additional correlation times on top of the subnanosecond ϕ_1 component for adequate fits to be obtained (Table 4). The fractional contribution of ϕ_2 and ϕ_3 was essentially independent of temperature, although their actual value changed considerably. From the parameters recorded in Table 4 the average order parameter of the probe and the apparent viscosity of the lipid bilayer were determined by the approaches and models described in Materials and Methods. These values are collected in Table 5 and discussed in detail below.

Resonance energy transfer from proteins to COPA

The utility of *t*-COPA incorporated into the lipid bilayers as an RET acceptor of protein tryptophan excitation was investigated by studying the RET of the couple gramicidin/*t*-COPA in LUVs of DMPC. The polypeptide gramicidin D shows no lipid specificity and inserts couple into phospholipid membranes to form a transient dimer spanning the bilayer (Wallace, 1990). The incorporation of the polypeptide into the membrane was monitored via the tryptophan absorption spectrum, recorded in the lipid suspension and in buffer alone, because this spectrum shifts 2 nm to the red in the lipid environment. In addition, the incorporation was confirmed by centrifuging the sample (120,000 × *g*) and

TABLE 4 Time-resolved fluorescence anisotropy parameters of *t*-COPA and *c*-COPA in paraffin oil and large unilamellar lipid vesicles of DMPC and POPC

	Solvent	T (°C)	β_1 (±0.03)	ϕ_1 (ns) (±0.1)	β_2 (±0.03)	ϕ_2 (ns) (±0.5)	β_3 (±0.03)	ϕ_3 (ns) (±0.5)	$\langle\phi\rangle$ (ns) (±0.5)	r_∞ (±0.006)	χ^2
t-COPA	Paraffin oil	22	0.31	0.1	0.27	4.1	0.42	14.1	7.1	—	1.15
		30	0.26	0.4	0.31	3.2	0.43	8.5	4.8	—	1.18
		39	0.21	<0.1	0.37	1.7	0.42	5.4	2.9	—	1.28
	DMPC	16	0.75	0.2	—	—	0.25	23.0	5.9	0.314	0.93
		25	0.33	0.1	0.29	1.0	0.38	6.9	2.9	0.128	0.94
		31	0.39	0.2	0.27	1.3	0.34	5.6	2.4	0.072	1.15
	POPC	10	0.38	0.2	0.29	2.5	0.33	15.5	5.9	0.075	1.06
		15	0.44	0.3	0.23	2.2	0.34	11.9	4.7	0.069	1.02
		20	0.32	0.1	0.36	1.6	0.33	10.1	3.9	0.063	1.07
		25	0.26	0.1	0.40	1.1	0.34	7.9	3.1	0.053	1.10
		30	0.31	<0.1	0.35	1.1	0.34	6.2	2.5	0.045	1.02
		40	0.21	<0.1	0.45	0.7	0.35	4.2	1.8	0.037	1.19
c-COPA	Paraffin oil	22	0.45	<0.1	0.19	2.8	0.36	10.1	4.2	—	1.28
	DMPC	16	0.58	0.3	—	—	0.42	17.4	7.5	0.301	1.02
		25	0.18	<0.1	0.43	1.0	0.39	7.1	3.2	0.122	1.08
		31	0.35	<0.1	0.38	1.3	0.27	6.4	2.3	0.050	1.19

subsequent resuspension of the pellet in a new buffer. The overlap between the gramicidin tryptophan emission and the *t*-COPA absorption spectra in the lipid gel phase is shown in Fig. 10; the overlap integral J for this system is 4.6×10^{14} $cm^3\ M^{-1}$. By taking values for the local refractive index of $n = 1.425$ (Toptygin and Brand, 1995), and for the protein intrinsic fluorescence quantum yield of $\Phi_D = 0.11$ (Wang et al., 1988), the computed R_o value would be 30 ± 2 Å, for the case in which the orientation factor $\kappa^2 = 2/3$. To measure the actual efficiency of energy transfer, aliquots of *t*-COPA in ethanol were added to a cuvette containing the suspension of DMPC/gramicidin vesicles, and the attenuation of the emission of tryptophan was recorded upon excitation at 260, 270 (Fig. 11), and 290 nm. The protein emission was quenched by the presence of *t*-COPA while, simultaneously, the fluorescence of the fatty acid induced by excitation in the tryptophan band increased, indicating transfer of the electronic excitation. The change in the shape of the emission spectrum of the protein observed at the higher *t*-COPA concentrations (Fig. 11) indicated that the absorption of the donor emission by acceptor molecules (radiative transport) also contributed to the apparent quenching of the protein fluorescence. By subtracting this contribution, quantified from the absorbance of the acceptor (Parker, 1968), the quenching of fluorescence exclusively due to the RET was determined to be 53% for the sample containing the highest concentration of *t*-COPA. The RET process between gramicidin and *t*-COPA was further substantiated by recording the excitation spectra of *t*-COPA in the DMPC/gramicidin samples and in peptide-free DMPC bilayers. The subtraction of the two spectra gave a *t*-COPA

TABLE 5 The order parameter, *S*, cone-model diffusion coefficient, and the "apparent" viscosity of the bilayer, η, calculated from the anisotropy parameters of Table 4

	Sample	T (°C)	S (±0.01)	$D_\perp$ (ns^{-1}) (±0.003)	η (poise) (±0.05)
t-COPA	DMPC	16	0.90	0.007	2.90
		25	0.58	0.043	0.46
		31	0.43	0.060	0.34
	POPC	10	0.44	0.025	0.77
		15	0.42	0.031	0.62
		20	0.40	0.038	0.52
		25	0.37	0.049	0.40
		30	0.34	0.061	0.33
		40	0.31	0.087	0.24
c-COPA	DMPC	16	0.88		
		25	0.56		
		31	0.36		

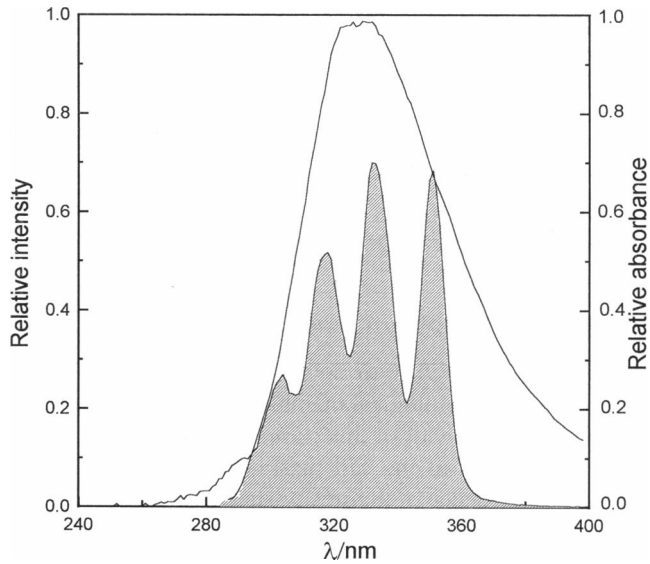

FIGURE 10 Spectral overlap between the tryptophan emission of gramicidin and the absorption spectrum of *t*-COPA in unilamellar vesicles of DMPC.

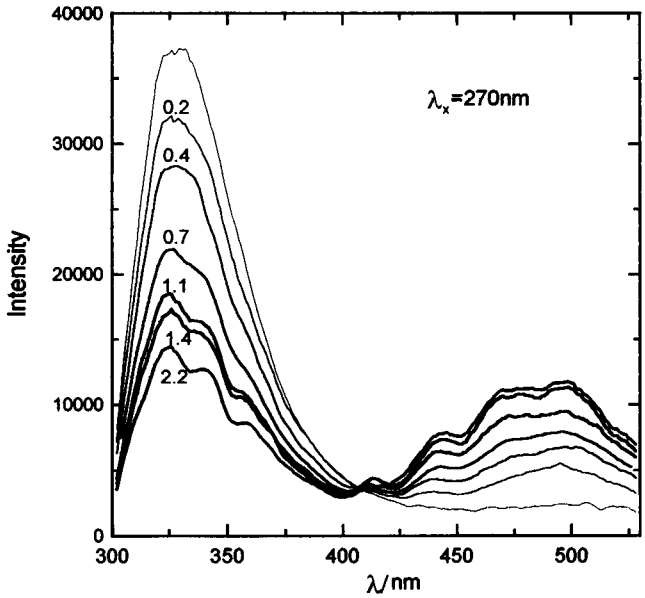

FIGURE 11 Emission spectra (λ_{exc} = 270 nm, 10°C) of gramicidin in DMPC unilamellar vesicles as a function of the indicated *t*-COPA/gramicidin molar ratio, showing the fluorescence of *t*-COPA at ~500 nm due to resonance energy transfer.

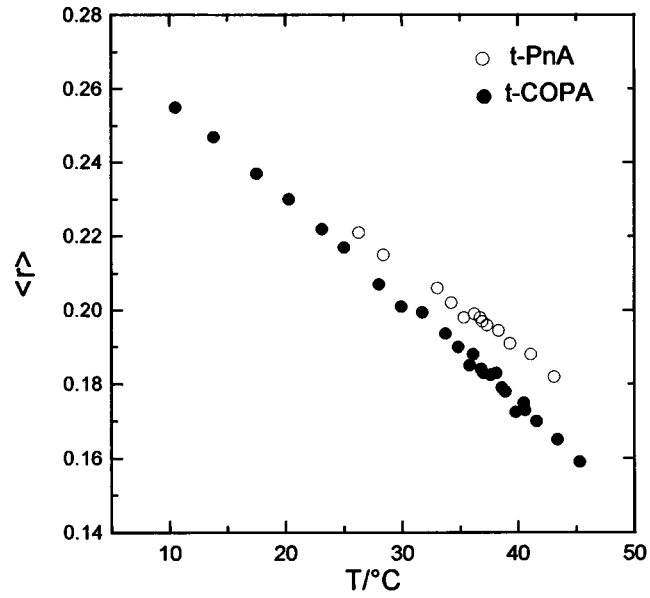

FIGURE 12 Temperature dependence of the steady-state fluorescence anisotropy of *t*-COPA and parinaric acid (*t*-PnA) in fragments of plasma membrane of human platelets.

fluorescence excitation spectrum containing the protein tryptophan band. A similar study was carried out for the lipid in the fluid phase with identical results.

The kinetic and equilibrium parameters of the complex formation between lipids and proteins with lipid-binding activity can also be accessed by means of the spectral properties of COPA derivatives. This is exemplified by the binding of *t*- and *c*-COPA to HSA, which gives rise to the enhancement of the fluorescence intensity of the probe and to the quenching (60%) of the intrinsic protein emission, due to RET between the albumin's single tryptophan and the polyene.

The spectral overlap integral J, determined for HSA-*t*-COPA and HSA-*c*-COPA from Eq. 12, were, respectively, 4.1×10^{14} cm^3 M^{-1} and 2.9×10^{14} cm^3 M^{-1}. By taking values for the refractive index of $n = 1.45$ (Berde et al., 1979), and for the protein fluorescence yield of $\Phi_D = 0.3$, the corresponding values of R_0 are 34 ± 2 Å for *t*-COPA and 32 ± 2 Å for *c*-COPA ($\kappa^2 = 2/3$).

Human platelet plasma membrane

The ability of *t*-COPA to detect changes in the physical properties of real biological membranes was investigated by recording the behavior of this compound in human platelets and in fragments of the cell plasma membrane. The temperature dependence of the steady-state fluorescence anisotropy $\langle r \rangle$ of *t*-COPA embedded in fragments of this membrane is shown in Fig. 12 and compared with that recorded for *t*-PnA in the same membrane (Mateo et al., 1991). The slope of the thermal change is the same for the two probes, although the absolute values of $\langle r \rangle$ are slightly higher for *t*-PnA. Because both probes should be located approximately at the same depth within the membrane, the difference in the anisotropy is probably due to the different fluorescence lifetime values, which are longer in *t*-COPA. The $\langle r \rangle$ values recorded in whole cells remained constant for several hours, indicating that *t*-COPA is not being internalized into other cell organelles.

DISCUSSION

Spectroscopy and dynamics of COPA in isotropic solvents

The major spectral properties of both COPA isomers are consistent with those observed in other linear polyenes (Hudson and Kohler, 1974; Hudson et al., 1982) and in the tetraene parinaric acids, the other polyenes used as membrane probes, although these pentaene and tetraene probes differ in several aspects, as emphasized below. The most relevant properties of the two COPA isomers related to their application as fluorescent probes are quite similar, and therefore the discussion will be focused on those of the most thoroughly studied isomer, the *trans* derivative *t*-COPA. Its strong, structured absorption band is red-shifted relative to that of parinaric acids because of the presence of an additional conjugated double bond, favoring those applications of COPA requiring its excitation in the presence of proteins. This band corresponds to the $1^1A_g \rightarrow 1^1B_u$ transition (Hudson and Kohler, 1974), that is, to the second excited singlet state, whereas the fluorescence originates from the forbidden transition $2^1A_g \rightarrow 1^1A_g$ (Hudson et al., 1982). In the conditions used in this work, emission from the state directly excited (1^1B_u), as reported for all(*E*)-2,4,6,8,10-do-

decapentaene in gas phase (Bouwman et al., 1990), was not observed. Because the strength of the emissive process is borrowed from the nearby allowed transition, the direction of the absorption and fluorescence transition moments should be the same (Hudson et al., 1982), as is indeed observed in the fluorescence polarization of both COPA isomers, which are characterized by a high r_0 value (0.385 ± 0.005).

In solvents of increasing refractive index, the absorption spectrum of *t*-COPA (but not that of fluorescence) shifts to lower energies. This solvent effect is usually explained in terms of polarizability interactions and is consistent with the involvement of two different electronic states in absorption and emission. The contraction of the volume surrounding the pentaene would give rise to a higher polarizability, thus shifting *t*-COPA absorption to the red. This property can be exploited in biological applications of this compound, as illustrated by the red shift observed in the fluid/gel phase transition of DMPC bilayers (Table 1).

The experimental radiative lifetime (Table 2) is at least two orders of magnitude larger than the value that can be obtained from the integrated absorption, as in parinaric acid, pointing again to the presence of the low-lying emitting state 2^1A_g. The kinetics of the fluorescence of *t*-COPA was biexponential in all the solvents studied here, with a dominant lifetime that, in ethanol at 20°C, is 11.4 ns (10 times larger than that of the tetraene analog) with a 90% fractional contribution to the decay. The minor component, 4.1 ns in this case, persisted even after extensive purification of the pentaenoic acid, and its origin is unknown. A similar biexponential kinetics is also recorded for solutions of the tetraene parinaric acid in similar solvents (see, e.g., Mateo et al., 1993a), and it has been suggested (Hudson et al., 1986) that this is due to the photogeneration of different conformers. If this were also the case for the COPA derivatives, the much slower decay constants of the pentaenoic acid afford a simpler experimental system to investigate that possibility.

A striking difference between the photophysics of COPA dyes and that of other polyenes—including parinaric acid—is the very weak temperature dependence of the radiationless rate processes of the pentaene in the 10–40°C range. The activation energy of the average k_{nr} of *t*-COPA is 1.0 kcal·mol^{-1}, compared with 5.3 kcal·mol^{-1} for *trans*-parinaric acid, facilitating considerably the use of the fluorescent emission of the pentaenes to monitor temperature-dependent membrane changes. A further, also unexplained, difference between the two types of polyenes is the large effect on the radiationless rate of changes in lipid packing density that characterizes the emission decay of the tetraenes (Sklar et al., 1977b; Hudson et al., 1986; Mateo et al., 1993a) but is not observed in the COPA isomers. These effects of temperature and lipid ordering on the photophysics of linear polyenes can only be unequivocally understood when the dominant radiationless channels are identified, which, unfortunately, is not yet the case.

The rotational dynamics of COPA isomers in paraffin oil, as detected by the decay of the emission anisotropy, contains features that can be interpreted by the superposition of rigid and flexible-body molecular motions. Thus the changes in the preexponential terms of the fast and intermediate correlation times when the viscosity decreases (Table 4) are most likely a consequence of fast conformational fluctuations of the saturated chain, such as *trans/gauche* changes. On the other hand, the slowest correlation time ϕ_3 changes with η/T in the way expected for rigid-body hydrodynamics, and its contribution to the total depolarizing kinetics is independent of η and T. Hence the diffusive motions of the probe may be modeled by those of a prolate ellipsoid of revolution in which the fast, subnanosecond conformational changes noted above do not substantially affect the overall tumbling of the molecule about axes perpendicular to the long inertial axis. In that case ϕ_3 is identified with $(6D_\perp)^{-1}$ (Rigler and Ehrenberg, 1973) and $D_\perp = 0.012$ ns^{-1} (*t*-COPA, paraffin oil, $\eta = 1.7$ poise, 22°C). Moreover, if the diffusive boundary conditions are closer to "slip" than to "stick" (Hu and Zwanzig, 1974), as in other lipophilic bilayer probes (Best et al., 1987; Mateo et al., 1993b), the dimensions of the equivalent ellipsoid, obtained by replacing the experimental $D_\perp$ value in Eq. 8, would be 18×6 Å, consistent with the *t*-COPA van der Waals volume. In a lipid bilayer, *t*-COPA molecules are anchored to the polar surface, and several of the conformations that are allowed in an isotropic solvent would be suppressed. Nevertheless, the overall tumbling rate may not be very different from that in the paraffin oil.

Probing physical parameters of lipid membranes with COPAs

We show here that the two COPA isomers align parallel to the bilayer lipids without perturbing the supramolecular structure. Furthermore, they distribute equally between solid and fluid domains, in contrast with the apparent preferential affinity of the related probe *trans*-parinaric acid for the most ordered phases. Giving the chemical structure of *t*-COPA and its photophysical characteristics, it is expected that the probe should report with fidelity the orientational order and dynamics of the surrounding lipid molecules. In fact, it is shown here that the probe steady-state fluorescence polarization accurately monitors the gel-fluid thermal lipid phase transition.

A measurement of the membrane equilibrium orientational order that depends on the effective orientational restoring potential can be obtained from the average second rank orientation parameter $\langle P_2 \rangle$, denoted usually as S. This may be determined by NMR, electron paramagnetic resonance, and fluorescence depolarization techniques to different degrees of approximation. Dynamic properties, on the other hand, depend on the diffusion coefficients of lipids as well as on the restoring potential.

The order parameter of the lipid chains, S_L, is, according to Best et al. (1987), the product of the parameter due

to the overall orientation of the chains, S_L^{rigid}, that is constant along the chain, and that corresponding to local conformational transitions, S_L^{conf}, which decrease toward the chain ends. Although S_L can be determined from deuterium NMR (Seelig and Seelig, 1980), extrinsic fluorescence probes may detect different values, depending on their structure, photophysics and transverse location in the bilayer. Using *t*-COPA, a probe that mimics the size, shape, and interactions of membrane lipids, a time-resolved anisotropy experiment allows a direct measurement of $S_{(COPA)}$ from the residual anisotropy via Eq. 3. To determine which kind of information this reports, we have summarized in Fig. 13 the order parameters of bilayers of POPC obtained from ^{2}H NMR (Lafleur et al., 1990), the spin-labeled lipids 1-palmitoyl-2-(16-doxylstearoyl)phosphatidylcholine (16PC) (Shin and Freed, 1989) and the 3-doxyl derivative of cholestan-3-one (CSL) (Van Ginkel et. al., 1986; Shin and Freed, 1989), and two fluorescence depolarization probes, 1,6-diphenyl-1,3,5-hexatriene (DPH) (Kinosita et al., 1984) and 1-[4-(trimethylamino)phenyl]-6-phenylhexa-1,3,5-triene (TMA-DPH) (Muller et al., 1994). It is shown that the parameter $S_{(COPA)}$ reproduces closely that observed with NMR techniques at the ninth carbon of the chain (Lafleur et al., 1990), as well as its temperature dependence. Because this carbon position is within the plateau region used in NMR experiments for determining the lipid order parameter (Seelig and Seelig, 1980), the *t*-COPA fluorescence depolarization monitors S_L. On the other hand, the rigid probe TMA-DPH gives $S = 0.51$, a too large value that probably reflects S_L^{rigid}. At the same temperature, the S_{DPH} value is close to that of *t*-COPA. However, it decreases drastically as the temperature increases, probably because of changes in DPH location within the bilayer. The spin probe cholestane (CSL) is rigid and anchored to the headgroup region of the bilayer and monitors a value similar to that of TMA-DPH, as expected, whereas the other spin probe with a nitroxide group in a distal position (16PC) shows a very low-order parameter.

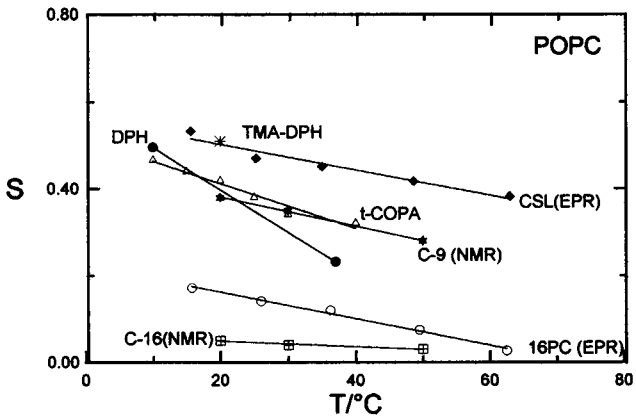

FIGURE 13 The order parameter of lipid bilayers of POPC as a function of temperature, as determined by deuterium NMR, electron paramagnetic resonance probes (CSL, 16PC), and fluorescence anisotropy (*t*-COPA, DPH, and TMA-DPH). See text for details.

The interpretation of the multiple correlation times of *t*-COPA in the lipid bilayers, spanning from hundreds of picoseconds to tens of nanoseconds, requires a model describing the restricted angular motion of the probe within the bilayer. Different models have been proposed to explain the decay of the anisotropy (Kinosita et al., 1977, 1982; Zannoni et al., 1983; Ameloot et al., 1984; Szabo, 1984), based on specific orienting potentials, which have attained only limited success. Recently, a new compound motion interpretation has been advanced (Van der Sijs et al., 1993; Muller et al., 1994), in which the reorientation of the probe results from the product of two separated motions, in the same vein as has been discussed above for lipid chain order parameters (Best et al., 1987). This approach is very appealing, but for the present purposes we have limited ourselves to the conceptual simplicity of the straightforward wobble-in-cone approximation (Kinosita et al., 1977, 1982) from which we obtained an average diffusion coefficient, $D_\perp$, for *t*-COPA by computation of the area under the decay curves. By referring the $D_\perp$ values to those of *t*-COPA measured in paraffin oil, estimates of the apparent viscosity of the lipid bilayers were determined. The values for DMPC bilayers, together with those estimated in the same way from the fluorescence depolarization of DPH and from the excimer formation of pyrene probes, are compared in Table 6. The three approaches yield similar viscosity values. On the other hand, when membrane proteins, such as bacteriorhodopsin or gramicidin, are used to monitor bilayer friction, very different values are determined, as is well known (Table 6). It is evident that this discrepancy arises from inherent differences between the interactions of the bilayer lipids with lipid-like probes (slip boundary conditions) and those with embedded proteins and peptides.

t-COPA as an acceptor of electronic excitation energy

In addition to its chemical properties, the large overlap between the emission from protein tryptophan residues and the *t*-COPA absorption spectrum, the high absorption coefficient, and a defined transverse location in lipid bilayers make this compound a suitable choice for RET experiments in membranes. As shown here, the large R_0 values (30–34 Å) calculated from the spectra lead to high transfer efficiencies not only in RET experiments involving a lipid-binding serum protein (HSA) in solution, but also from the channel-forming membrane peptide gramicidin to the probe in bilayer membranes. Interestingly, the transfer efficiency in the latter case was independent of whether the lipid bilayer was in the fluid or the gel phase, suggesting that the relative distribution of the peptide and the probe is the same under either condition. Finally, it should be noted that the R_0 values reported

TABLE 6 Apparent viscosities for DMPC bilayers

Technique	T (°C)	η (poise)	Reference
Fluorescence depolarization			
t-COPA	16	2.90	This work
	25	0.46	This work
	31	0.34	This work
DPH	10	2.39	Kinosita et al. (1984)
	35	0.27	Kinosita et al. (1984)
	35	0.2	Best et al. (1987)
Intramolecular excimer (dipyrenylpropane)	37	0.23	Zachariasse et al. (1982)
	10–60	1.25–0.38	Zachariasse et al. (1980)
Intermolecular excimer (pyrene)	30	0.59	Vanderkooi and Callis (1974)
^{2}H-NMR (deuterated gramicidin)	35	1.7	Macdonald and Seelig (1988)
Time-resolved dichroism (bacteriorhodopsin)	25–37	3.7 ± 1.3	Cherry and Godfrey (1981)

here were computed on the assumption of dynamic random averaging of the RET orientation factor (i.e., $\kappa^2 = 2/3$). The validity of this assumption was assessed, in the case of gramicidin, by measuring the emission anisotropy $\langle r \rangle$ of the peptide donor. The experimental value was quite low (0.07), consistent with a high rotational freedom of the emitting tryptophan residues and, hence, a small deviation of the above R_0 value from the correct one.

CONCLUSIONS

The conjugated linear octadecapentaenoic acids studied here, *t*- and *c*-COPA, have large molar absorption coefficients in a convenient spectral range for their application to probe natural membranes and cells, with which protein tryptophan emission shows extensive overlap. In nonpolar solvents, these molecules emit fluorescence, strongly polarized if the solvents are viscous, with reasonable yields, a large Stokes shift, and long lifetimes. The kinetics of the fluorescence emission does not depend on the temperature in the 10–40°C range. In addition, both isomers incorporate into lipid membranes in a well-defined transverse location with negligible perturbation of the bilayer structure and distribute equally between fluid and solid domains of bilayers of DMPC and DPPC. The fraction that remains in the water solution is negligible and nonfluorescent. From the variety of experiments reported here, it is shown that the use of COPA isomers presents clear advantages in the monitoring of the order and fluidity of synthetic and natural membranes, and in determining proximity relationships between tryptophan-containing soluble and membrane proteins and lipids. It appears that these fluorescent fatty acids could be of great utility in the examination of lipid bilayer structure and dynamics and of lipid interactions.

We thank Dr. M. P. Lillo for developing the deconvolution programs used in this work, Dr. J. Laynez for the DSC measurements of lipid vesicles, and Dr. J. González and G. Pinillos for help in the preparation of platelet membranes. Helpful discussions at the early stages of this work with Drs. M. E. Prieto and A. Coutinho (I. S. T., Lisbon) are also gratefully acknowledged. The critical reading of the manuscript by Dr. R. E. Dale was invaluable.

Financial support was provided by the Dirección General de Investigación Científica y Técnica (Spain), project PB93-0126. CRM was supported by a DGICYT research contract, and AAS by a predoctoral grant from the CNPq (Brazil).

REFERENCES

Ameloot, M., H. Hendrickx, W. Herreman, H. Pottel, F. V. Cauwelaert, and B. W. Van der Meer. 1984. Effect of orientational order on the decay of the fluorescence anisotropy in membrane suspensions. *Biophys. J.* 46:525–539.

Bañó, M. C., L. Braco, and C. Abad. 1991. Conformational transitions of gramicidin A in phospholipid model membranes. A high-performance liquid chromatography assessment. *Biochemistry.* 30:886–894.

Berde, C., B. S. Hudson, R. D. Simoni, and L. A. Sklar. 1979. Human serum albumin. Spectroscopic studies of binding and proximity relationships for fatty acids and bilirubin. *J. Biol. Chem.* 254:391–400.

Best, L., E. John, and F. Jähnig. 1987. Order and fluidity of lipid membranes as determined by fluorescence anisotropy decay. *Eur. Biophys. J.* 15:87–102.

Bouwman, W. G., A. C. Jones, D. Phillips, P. Thibodeau, C. Friel, and R. L. Christensen. 1990. Fluorescence of gaseous tetraenes and pentaenes. *J. Phys. Chem.* 94:7429–7434.

Castanho, M., and M. E. Prieto. 1995. Filipin fluorescence quenching by spin-labelled probes. Studies in aqueous solution and in a membrane model system. *Biophys. J.* 69:155–168.

Castanho, M., M. E. Prieto, and A. U. Acuña. 1996. The transverse location of the fluorescence probe *trans*-parinaric acid in lipid bilayers. *Biochim. Biophys. Acta.* 1279:164–168.

Chattopadhyay, A., and E. London. 1987. Parallax method for direct measurement of membrane penetration depth utilising fluorescence quenching by spin-labelled phospholipids. *Biochemistry.* 26:39–45.

Cherry, R. J., and R. E. Godfrey. 1981. Anisotropic rotation of bacteriorhodopsin in lipid membranes. *Biophys. J.* 36:257–276.

Cross, A. J., and G. R. Fleming. 1984. Analysis of time-resolved fluorescence anisotropy decays. *Biophys. J.* 46:45–56.

Dale, R. E., L. A. Chen, and L. Brand. 1977. Rotational relaxation of the "microviscosity" probe diphenylhexatriene in paraffin oil and egg lecithin vesicles. *J. Biol. Chem.* 252:7500–7510.

Dote, J. L., D. Kivelson, and R. N. Schwartz. 1981. A molecular quasi-hydrodynamic free-space model for molecular rotational relaxation in liquids. *J. Phys. Chem.* 85:2169.

Engel, L. W., and F. G. Prendergast. 1981. Values for and significance of order parameters and "cone angles" of fluorophore rotation in lipid bilayers. *Biochemistry.* 20:7338–7345.

Förster, T. 1959. Transfer mechanism of electronic excitation. *Discuss. Faraday Soc.* 27:7–17.

Heyn, M. P. 1989. Order and viscosity of membranes. Analysis by time-resolved fluorescence depolarization. *Methods Enzymol.* 172:462–471.

Hope, M. J., M. B. Bally, G. Webb, and P. R. Cullis. 1985. Production of large unilamellar vesicles by a rapid extrusion procedure. Characterization of size distribution, trapped volume and ability to maintain a membrane potential. *Biochim. Biophys. Acta.* 812:55–65.

Hu, C. M., and R. Zwanzig. 1974. Rotational friction coefficients for spheroids with the slipping boundary condition. *J. Chem. Phys.* 60: 4354–4357.

Hudson, B. S., and S. Cavalier. 1988. Studies of membrane dynamics and lipid-protein interactions with parinaric acid. *In* Spectroscopic Membrane Probes, Vol. 1. L. M. Loew, editor. CRC Press, Boca Raton, FL. 43–62.

Hudson, B. S., D. L. Harris, R. D. Ludescher, A. Ruggiero, A. Cooney-Fred, and S. A. Cavalier. 1986. Fluorescence probe studies of protein and membranes. *In* Applications of Fluorescence in the Biomedical Sciences. D. L. Taylor, A. S. Waggoner, F. Lanni, R. F. Murphy, and R. Birge, editors. Alan R. Liss, New York. 159–202.

Hudson, B., and B. Kohler. 1974. Linear polyene structure and spectroscopy. *Annu. Rev. Phys. Chem.* 25:437–460.

Hudson, B. S., B. E. Kohler, and K. Schulten. 1982. Linear polyene electronic structure and potential surfaces. *In* Excited States, Vol. 6. E. C. Lim, editor. Academic Press, New York. 1–95.

Kimelman, D., E. S. Tecona, P. K. Wolber, B. S. Hudson, W. T. Wickner, and R. D. Simoni. 1979. Protein-lipid interactions. Studies of M13 coat protein in dimyristoylphosphatidylcholine vesicles using parinaric acid. *Biochemistry.* 18:5874–5880.

Kinosita, K., Jr., A. Ikegami, and S. Kawato. 1982. On the wobbling-in-cone analysis of fluorescence anisotropy decay. *Biophys. J.* 37:461–464.

Kinosita, K., Jr., S. Kawato, and A. Ikegami. 1977. A theory of fluorescence polarization decay in membranes. *Biophys. J.* 20:289–305.

Kinosita, K., Jr., S. Kawato, and A. Ikegami. 1984. Dynamic structure of biological and model membranes: analysis by optical anisotropy decay measurements. *Adv. Biophys.* 17:147–203.

Knutson, J. R., J. M. Beechem, and L. Brand. 1983. Simultaneous analysis of multiple fluorescence decay curves: a global approach. *Chem. Phys. Lett.* 102:501–507.

Lafleur, M., P. R. Cullis, and M. Bloom. 1990. Modulation of the orientational order profile of the lipid acyl chain in the L_α phase. *Eur. Biophys. J.* 19:55–62.

Lentz, B. R. 1993. Use of fluorescent probes to monitor molecular order and motions within liposome bilayers. *Chem. Phys. Lipids.* 64:99–116.

Lipari, G., and A. Szabo. 1980. Effect of librational motion on fluorescence depolarization and nuclear magnetic resonance relaxation in macromolecules and membranes. *Biophys. J.* 30:489–506.

Löfroth, J. E. 1985. Deconvolution of single photon counting data with a reference method and global analysis. *Eur. Biophys. J.* 13:45–48.

Lograsso, P. V., F. Moll, and T. A. Cross. 1988. The solvent history dependence of gramicidin A conformations in hydrated lipid bilayers. *Biophys. J.* 54:259–267.

López, M. C., and J. García de la Torre. 1987. Brownian dynamics simulation of restricted rotational diffusion. *Biophys. J.* 52:303–310.

Mabrey, S., and M. Sturtevant. 1976. Investigation of phase transitions of lipids and lipid mixtures by high sensitivity differential scanning calorimetry. *Proc. Natl. Acad. Sci. USA.* 73:3862–3866.

Macdonald, P. M., and J. Seelig. 1988. Dynamic properties of gramicidin A in phospholipid membranes. *Biochemistry.* 27:2357–2364.

Mateo, C. R., A. U. Acuña, and J. C. Brochon. 1995. Liquid-crystalline phases of cholesterol/lipid bilayers as revealed by the fluorescence of *trans*-parinaric acid. *Biophys. J.* 68:978–987.

Mateo, C. R., J. C. Brochon, M. P. Lillo, and A. U. Acuña. 1993a. Lipid clustering in bilayers detected by the fluorescence kinetics and anisotropy of *trans*-parinaric acid. *Biophys. J.* 65:2237–2247.

Mateo, C. R., M. P. Lillo, J. C. Brochon, M. Martínez-Ripoll, J. Sanz-Aparicio, and A. U. Acuña. 1993b. Rotational dynamics of 1,6-diphenyl-1,3,5-hexatriene and derivatives from fluorescence depolarization. *J. Phys. Chem.* 97:3486–3491.

Mateo, C. R., M. P. Lillo, J. González-Rodriguez, and A. U. Acuña. 1991. Molecular order and fluidity of the plasma membrane of human platelets from time-resolved fluorescence depolarization. *Eur. Biophys. J.* 20: 41–52.

Mukherjee, S., and A. Chattopadhyay. 1994. Motionally restricted tryptophan environments at the peptide-lipid interface of gramicidin channels. *Biochemistry.* 33:5089–5097.

Muller, J. M., E. E. van Faassen, and G. van Ginkel. 1994. Experimental support for a novel compound motion model for the time-resolved fluorescence anisotropy decay of TMA-DPH in lipid vesicle bilayers. *Chem. Phys.* 185:393–404.

Naqvi, K. R. 1980. Photoselection in uniaxial liquid crystals: the effect of rotational Brownian motion on measurements of orientational distribution function. *J. Chem. Phys* 73:3019–3020.

Naqvi, K. R. 1981. Photoselection in uniaxial liquid crystals: the advantages of using saturating light pulses for the determination of orientational order. *J. Chem. Phys.* 74:2658–2659.

Naqvi, K. R., and A. U. Acuña. 1992. Polarized radiation and dynamics of biological systems. *In* Computational Chemistry: Structure, Interactions and Reactivity, Part B. S. Fraga, editor. Elsevier Science Publishers, Amsterdam. 246–267.

Parker, C. A. 1968. Photoluminescence of Solutions. Elsevier Publishing Company, Amsterdam. 222.

Rigler, R., and M. Ehrenberg. 1973. Molecular interactions and structure as analysed by fluorescence spectroscopy. *Q. Rev. Biophys.* 6:139–199.

Ruggiero, A., and B. Hudson. 1989a. Critical density fluctuations in lipid bilayers detected by fluorescence lifetime heterogeneity. *Biophys. J.* 55:1111–1124

Ruggiero, A., and B. Hudson. 1989b. Analysis of the anisotropy decay of *trans*-parinaric acid in lipid bilayers. *Biophys. J.* 55:1125–1135.

Seelig, J., and A. Seelig. 1980. Lipid conformation in model membranes and biological membranes. *Q. Rev. Biophys.* 13:19–61.

Shin, Y.-K., and J. H. Freed. 1989. Dynamic imaging of lateral diffusion by electron spin resonance and study of rotational dynamics in model membranes. *Biophys. J.* 55:537–550.

Sklar, L. A. 1980. The partition of *cis*-parinaric acid and *trans*-parinaric acid among aqueous, fluid lipid and solid lipid phases. *Mol. Cell. Biochem.* 32:169–177.

Sklar, L. A., B. S. Hudson, M. Petersen, and J. Diamond. 1977a. Conjugated polyene fatty acids as fluorescent probes: spectroscopic characterisation. *Biochemistry.* 16:813–818.

Sklar, L. A., B. S. Hudson, and R. D. Simoni. 1977b. Conjugated polyene fatty acids as fluorescent probes: synthetic phospholipid membrane studies. *Biochemistry.* 16:819–828.

Sklar, L. A., G. P. Miljanich, S. L. Bursten, and E. A. Dratz. 1979. Thermal lateral phase separations in bovine retinal rod outer segment membranes and phospholipids as evidenced by parinaric acid fluorescence polarization and energy transfer. *J. Biol. Chem.* 254:9583–9591.

Souto, A. A., A. U. Acuña, and F. Amat-Guerri. 1994. A general and practical synthesis of linear conjugated pentaenoic acids. *Tetrahedron Lett.* 32:5907–5910.

Szabo, A. 1984. Theory of polarized fluorescent emission in uniaxial liquid crystals. *J. Chem. Phys.* 72:4620–4626.

Toptygin, D., and L. Brand. 1995. Determination of DPH order parameters in unoriented vesicles. *J. Fluorescence.* 5:39–50.

Valeur, B. 1993. Fluorescent probes for evaluation of local physical and structural parameters. *In* Molecular Luminescence Spectroscopy, Part 3. S. G. Schulman, editor. John Wiley and Sons, New York. 25–84.

Vanderkooi, J., and J. B. Callis. 1974. Pyrene. A probe of lateral diffusion in the hydrophobic region of membranes. *Biochemistry.* 13:4000–4006.

Van der Meer, B. W. 1991. "Membrane fluidity," more than one single parameter. *Acta Pharm. Jugosl.* 41:311–326.

Van der Meer, B. W., G. Coker III, and S. Y. S. Chen. 1994. Resonance Energy Transfer. Theory and Data. VCH Publishers, New York.

Van der Sijs, D. A., E. E. van Faassen, and Y. K. Levine. 1993. The interpretation of the fluorescence anisotropy decays of probe molecules in membrane systems. *Chem. Phys. Lett.* 216:559–565.

Van Ginkel, G., L. J. Korstanje, H. van Langen, and Y. K. Levine. 1986. The correlation between molecular orientational order and reorientational dynamics of probe molecules in lipid multibilayers. *Faraday Discuss. Chem. Soc.* 81:49–61.

Velapoldi, R. A. 1972. Considerations on organic compounds in solution and inorganic ions in glasses as fluorescent standard reference materials. *J. Res. Natl. Bur. Stand. (U.S.).* 76A:641–654.

Wallace, B. A. 1990. Gramicidin channels and pores. *Annu. Rev. Biophys. Biophys. Chem.* 19:127–157.

Wang, S., E. Martin, J. Cimino, G. Omann, and M. Glaser. 1988. Distribution of phospholipids around gramicidin and D-β-hydrohybutyrate dehydrogenase as measured by resonance energy transfer. *Biochemistry.* 27:2033–2039.

Wardlaw, J. R., W. H. Sawyer, and K. P. Ghiggino. 1987. Vertical fluctuation of phospholipid acyl chains in bilayers. *FEBS Lett.* 231: 20–24.

Zachariasse, K. A., W. Kühnle, and A. Weller. 1980. Intramolecular excimer fluorescence as a probe of fluidity changes and phase transitions in phosphatidylcholine bilayers. *Chem. Phys. Lett.* 73:6–11.

Zachariasse, K. A., W. L. C. Vaz, C. Sotomayor, and W. Kühnle. 1982. Investigation of human erythrocyte ghost membranes with intramolecular excimer probes. *Biochim. Biophys. Acta.* 688:323–332.

Zannoni, C., A. Arcioni, and P. Cavatorta. 1983. Fluorescence depolarization in liquid crystals and membrane bilayers. *Chem. Phys. Lipids.* 32:179–250.